MOLECULAR AND CELLULAR BIOLOGY, Apr. 1994, p. 2447–2456
0270-7306/94/$04.00+0

Vol. 14, No. 4

rac p21 Is Involved in Insulin-Induced Membrane Ruffling and *rho* p21 Is Involved in Hepatocyte Growth Factor- and 12-*O*-Tetradecanoylphorbol-13-Acetate (TPA)-Induced Membrane Ruffling in KB Cells

TAKAYUKI NISHIYAMA,[1]† TAKUYA SASAKI,[1]‡ KENJI TAKAISHI,[1]‡ MASAKI KATO,[1]‡ HIDEAKI YAKU,[1]§ KEISHI ARAKI,[1]‡ YOSHIHARU MATSUURA,[2] AND YOSHIMI TAKAI[1,3]*

Department of Biochemistry, Kobe University School of Medicine, Kobe 650,[1] Department of Virology II, National Institute of Health, Tokyo 208,[2] and Department of Cell Physiology, National Institute for Physiological Sciences, Okazaki 444,[3] Japan

Received 20 September 1993/Returned for modification 21 October 1993/Accepted 19 January 1994

Insulin and hepatocyte growth factor (HGF) induced morphologically different membrane rufflings in KB cells. Insulin-induced membrane ruffling was inhibited by microinjection of *rho* GDI, an inhibitory GDP/GTP exchange regulator for both *rho* p21 and *rac* p21 small GTP-binding proteins, but not inhibited by microinjection of botulinum exoenzyme C3, known to selectively ADP-ribosylate *rho* p21 and to impair its function. This *rho* GDI action was prevented by comicroinjection with guanosine 5′-(3-*O*-thio)triphosphate (GTPγS)-bound *rac*1 p21. In contrast, HGF-induced membrane ruffling was inhibited by microinjection of *rho* GDI or C3. This *rho* GDI action was prevented by comicroinjection with GTPγS-bound *rho*A p21, and this C3 action was prevented by comicroinjection with GTPγS-bound *rho*A^{Ile-41} p21, which is resistant to C3. Microinjection of either GTPγS-bound *rac*1 p21 or *rho*A p21 alone induced membrane ruffling in the absence of the growth factors. The *rac*1 p21-induced membrane ruffling was morphologically similar to the insulin-induced kind, whereas *rho*A p21-induced ruffling was apparently different from both the insulin- and HGF-induced kinds. Membrane ruffling was also induced by 12-*O*-tetradecanoylphorbol-13-acetate (TPA), a protein kinase C-activating phorbol ester, but not by Ca^{2+} ionophore or microinjection of a dominant active Ki-*ras* p21 mutant (Ki-*ras*$^{Val-12}$ p21). The phorbol ester-induced membrane ruffling was morphologically similar to the *rho*A p21-induced kind and inhibited by microinjection of *rho* GDI or C3. These results indicate that *rac* p21 and *rho* GDI are involved in insulin-induced membrane ruffling and that *rho* p21 and *rho* GDI are involved in HGF- and phorbol ester-induced membrane rufflings.

Membrane ruffling is rapid movement with irregular fluctuation of protrusion and withdrawal of the margin of the cell surface and is believed to be associated with spreading and locomotion in cultured cells (1, 17). The molecular events responsible for the ruffling formation are not known, but it has been suggested to be caused by a polymerization of actin at the inner surface of the plasma membrane (32). It is known that various growth factors induce morphologically different membrane rufflings in various types of cells (20, 26, 27, 32, 34, 43). For instance, KB cells, a cell strain derived from human epidermoid carcinoma, form membrane ruffling in response to insulin, insulin-like growth factor I, and epidermal growth factor (EGF) (20, 26, 27, 34). Insulin- and insulin-like growth factor I-induced membrane rufflings of KB cells are visible as irregular rims along a part or around all of the margin of the cells. In contrast, EGF-induced ruffling is visible as curtain-like folds or rod-like spikes (27). Human fibroblasts form circular membrane ruffling in response to platelet-derived growth factor (PDGF) (32). These growth factors are known to induce a number of rapid biological responses, including an increase in receptor-associated tyrosine kinase activity, phosphoinositide turnover associated with production of diacylglycerol and inositol triphosphate, and intracellular Ca^{2+} mobilization (for a review, see reference 12). However, it is not known at present which, if any, of these receptor-mediated signals is involved in growth factor-induced membrane rufflings.

It has recently been reported that *rac*1 p21 regulates membrane ruffling induced by PDGF, EGF, and insulin in Swiss 3T3 cells (43). *rac*1 p21 is a member of the *rho* family which belongs to the small GTP-binding protein (G protein) superfamily (15; for reviews, see references 23 and 52). The *rho* family consists of the *rac*, *rho*, and G25K subfamilies. The *rac* subfamily consists of two members, *rac*1 and *rac*2 p21s, and regulates not only membrane ruffling in Swiss 3T3 cells but also NADPH oxidase-catalyzed superoxide formation in neutrophils (2, 7, 31, 35, 44). The *rho* subfamily consists of three members, *rho*A, *rho*B, and *rho*C p21s, and only this subfamily is ADP-ribosylated by *Clostridium botulinum* ADP-ribosyltransferase C3 (6, 10, 29, 38, 39). C3 ADP-ribosylates Asn-41 of *rho* p21, which is located in the putative effector domain (50), and the ADP-ribosylation impairs the functions of *rho* p21. Evidence that *rho* p21 regulates various actomyosin-dependent cell functions, such as cell morphology (14, 33, 41, 42, 45), smooth-muscle contraction (25), platelet aggregation (36), cell motility (53, 54), cytokinesis (30), and lymphocyte aggregation (55), is accumulating. We have recently shown that

* Corresponding author. Present address: Department of Molecular Biology and Biochemistry, Osaka University Medical School, 2-2 Yamada-oka, Suita 565, Japan. Phone: 81-6-879-3410. Fax: 81-6-879-3419.

† Present address: Department of Orthopedic Surgery, Kobe University School of Medicine, Kobe 650, Japan.

‡ Present address: Department of Molecular Biology and Biochemistry, Osaka University Medical School, Suita 565, Japan.

§ Present address: Department of Anesthesiology, Kobe University School of Medicine, Kobe 650, Japan.

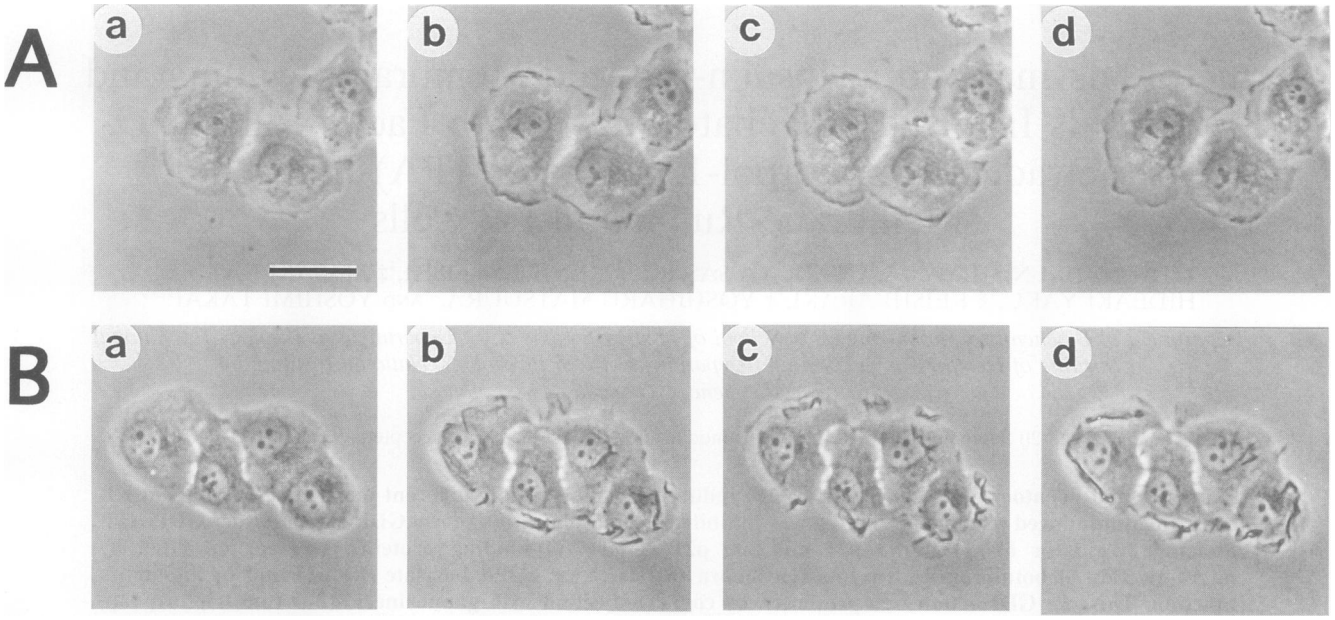

FIG. 1. Time courses of insulin- and HGF-induced membrane rufflings of KB cells. KB cells were stimulated with 1×10^{-6} M insulin (A) or 5×10^{-11} M HGF (B). Photographs were taken 0 min (a), 5 min (b), 10 min (c), and 30 min (d) after stimulation with each growth factor. The results shown are representative of three independent experiments. Bar, 20 μm. All photographs were taken with the same magnification.

rho p21 is involved in the hepatocyte growth factor (HGF)- and protein kinase C (PKC)-activating phorbol ester-induced cell motility in mouse keratinocytes (54).

These functions of *rho* p21 strongly suggest that *rho* p21 is also involved in membrane ruffling, but it has been shown that *rho* p21 is not involved in membrane ruffling induced by PDGF, EGF, or insulin in Swiss 3T3 cells (43). Therefore, we have investigated here a possible involvement of *rho* p21 in membrane ruffling of another type of cells, KB cells. We have first examined whether HGF also induces membrane ruffling in this cell type and found that it induces membrane ruffling morphologically different from the insulin-induced kind. Then, we have examined whether *rho* p21 is involved in insulin- and HGF-induced membrane rufflings. For this purpose, we have utilized C3 and *rho* GDI. *rho* GDI is an inhibitory GDP/GTP exchange regulator specific for the *rho* family (7, 19, 24, 35, 56). *rho* GDI forms a stoichiometric complex with the GDP-bound form of each *rho* family member preferentially to forming one with the GTP-bound form and thereby inhibits its conversion from the GDP-bound form to the GTP-bound form (48, 56). We have found here that *rho* p21 is involved in HGF-induced membrane ruffling, although *rac* p21 is involved in the insulin-induced kind. We have moreover found here that PKC-activating phorbol ester induces membrane ruffling and that *rho* p21 is also involved in this membrane ruffling.

MATERIALS AND METHODS

Materials and chemicals. KB cells were kindly supplied by Y. Miyata, Tokyo Metropolitan Institute of Medical Science, Tokyo, Japan (34). Insulin and 12-*O*-tetradecanoylphorbol-13-acetate (TPA) were obtained from Sigma Chemical Co. Human recombinant HGF, which was purified from culture fluid of C-127 cells, was kindly supplied by T. Nakamura, Osaka University, Osaka, Japan (37). The cDNAs of *rho*A p21 and Ki-*ras*$^{Val\text{-}12}$ p21 were kindly provided by P. Madaule, Centre National de la Recherche Scientifique, Gif sur Yvette, France, and R. A. Weinberg, Massachusetts Institute of Technology, Boston, respectively. The cDNA of *rac*1 p21 was kindly provided by P. Polakis and F. McCormick, Onyx Pharmaceuticals, Richmond, Calif. C3 was kindly supplied from S. Narumiya, Kyoto University, Kyoto, Japan (39). Mutagenesis of Ser to Asn at codon 17 of Ki-*ras* p21 (Ki-*ras*$^{Asn\text{-}17}$ p21) and mutagenesis of Asn to Ile at codon 41 of *rho*A p21 (*rho*A$^{Ile\text{-}41}$ p21) were carried out by site-directed mutagenesis (47). *rho*A p21, *rho*A$^{Ile\text{-}41}$ p21, *rac*1 p21, Ki-*ras*$^{Val\text{-}12}$ p21, or Ki-*ras*$^{Asn\text{-}17}$ p21 was expressed in *Spodoptera frugiperda* cells (Sf9 cells) by using the insect-baculovirus system and purified from the cytosol fraction of the cells overexpressing each small G protein as described elsewhere (30, 33, 53, 54). *rho* GDI was purified as a glutathione *S*-transferase fusion protein from *Escherichia coli* which overexpressed glutathione *S*-transferase–*rho* GDI as described previously (51). Active protein concentrations of these small G proteins were determined by their [^{35}S]guanosine 5′-(3-*O*-thio)triphosphate (GTPγS)-binding activity, which was assayed by the filtration method as described previously (56). GTPγS-bound *rho*A p21, *rho*A$^{Ile\text{-}41}$ p21, and *rac*1 p21 were made by incubating each small G protein with 60 μM GTPγS as described previously (33, 53, 54). All the proteins used were concentrated to 2 to 20 mg/ml with Centricon-10 (Amicon). During the concentration, the buffers contained in the same sample preparations were replaced by buffer A (20 mM Tris-HCl [pH 7.4] containing 20 mM NaCl, 2 mM $MgCl_2$, 100 μM ATP, 0.1 mM EDTA, and 1 mM 2-mercaptoethanol). Fluorescein isothiocyanate (FITC)-labeled phalloidin was obtained from Sigma Chemical Co. Other materials and chemicals were obtained from commercial sources.

Analysis of membrane rufflings. Stock cultures of KB cells were maintained at 37°C in a humidified atmosphere of 5% CO_2 and 95% air in Dulbecco's modified Eagle's medium containing 10% fetal calf serum (GIBCO), penicillin (100 U/ml), and streptomycin (100 μg/ml). KB cells were seeded on 35-mm-diameter grid tissue culture dishes (Nunc Inc.) at a

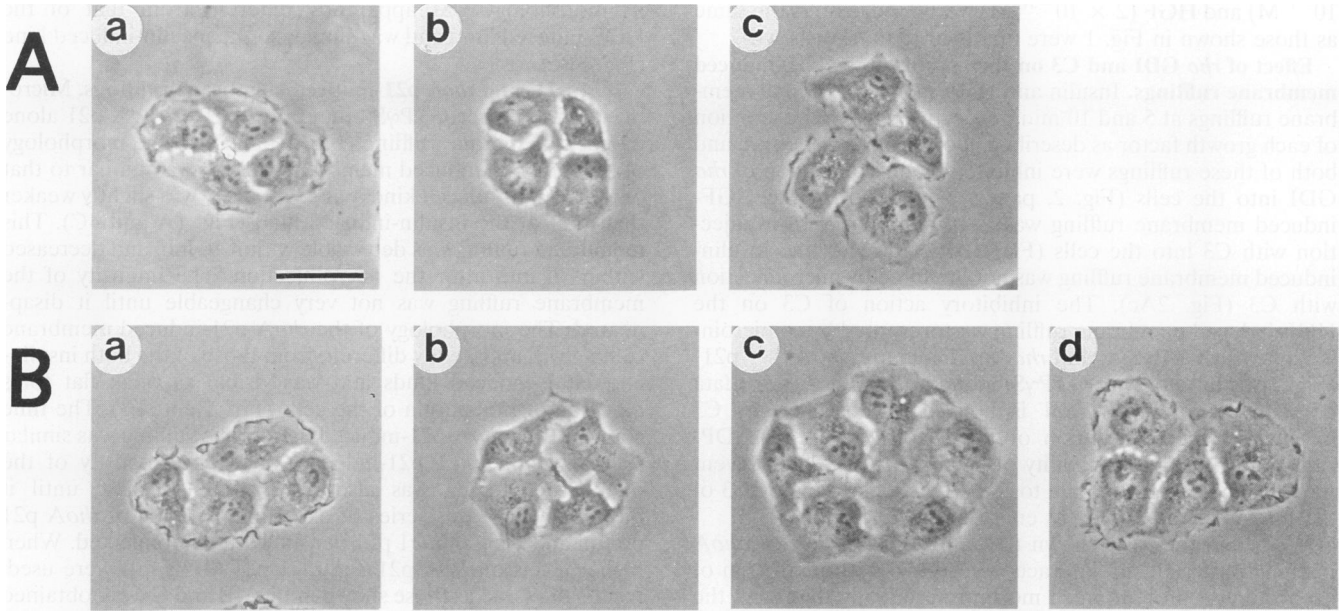

FIG. 2. Inhibition of insulin- and HGF-induced membrane rufflings by microinjection of *rho* GDI or C3 into KB cells. KB cells were microinjected with buffer A (a), *rho* GDI (b), C3 (c), or C3 plus GTPγS-bound *rho*A^{Ile-41} p21 (d). At 30 min after microinjection, KB cells were stimulated with 1×10^{-6} M insulin (A) or 5×10^{-11} M HGF (B). Photographs were taken 5 min after stimulation with insulin and 10 min after stimulation with HGF. The results shown are representative of three independent experiments. Bar, 20 μm. All photographs were taken with the same magnification.

density of 10^4 cells per dish in 1 ml of Dulbecco's modified Eagle's medium containing 10% fetal calf serum and were incubated for 3 days. Then, the medium was changed to serum-free Dulbecco's modified Eagle's medium and the cells were further incubated for 36 h. After the incubation, microinjection was performed, and insulin, HGF, or TPA was added. Membrane ruffling was analyzed with a phase-contrast microscope (model IMT-2; Olympus, Tokyo, Japan). Photographs were taken at various intervals after the addition of growth factors, microinjection, or both. The membrane ruffling was also analyzed with a fluorescence microscope (model Axiophot; Carl Zeiss, Oberkochen, Germany) after filamentous actin (F-actin) staining with FITC-labeled phalloidin. For this series of experiments, cells grown on glass coverslips were washed with phosphate-buffered saline (PBS) and fixed in 3.7% formaldehyde–PBS for 30 min at room temperature. About 200 μl of 2-μg/ml FITC-labeled phalloidin was applied to each coverslip. After the coverslips were incubated in a humidified chamber for 60 min at 37°C, they were washed in PBS and mounted in 20% glycerol–PBS containing 1 mg of *p*-phenylenediamine per ml, and the edges were sealed with nail polish. These samples were then examined by fluorescence microscopy.

Microinjection. Each sample to be tested was microinjected into living KB cells as previously described (8, 58). Briefly, glass capillaries drawn to a tip diameter of less than 1 μm were used to microinject each sample. About 50 cells were usually microinjected within 5 min at 36 h after the cells were serum starved. About 5×10^{-14} liter of sample was microinjected by one injection. When GTPγS-bound *rho*A p21, GTPγS-bound *rho*A^{Ile-41} p21, GTPγS-bound *rac*1 p21, Ki-*ras*$^{Val-12}$ p21, or Ki-*ras*$^{Asn-17}$ p21 was microinjected at 1 mg/ml, the intracellular concentration of microinjected samples was calculated to be about 7 μM. Since the endogenous concentration of *rho*A p21, *rac*1 p21, or Ki-*ras* p21 is not known, the levels of the exogenous and endogenous small G proteins were not compared. When glutathione *S*-transferase–*rho* GDI was microinjected at 5 mg/ml, its intracellular concentration was about 13 μM. The intracellular concentration of the microinjected *rho* GDI was about 40-fold higher than its endogenous level. C3 was microinjected at 130 μg/ml, and its intracellular concentration was about 0.74 μM.

Determination of protein concentrations. Protein concentrations were determined with bovine serum albumin as a standard by densitometric tracing of protein bands stained with Coomassie brilliant blue on a sodium dodecyl sulfate-polyacrylamide gel as described elsewhere (57).

RESULTS

Insulin- and HGF-induced membrane rufflings in KB cells. Growth factor-induced membrane ruffling was visible as phase-dark regions in KB cells by phase-contrast microscopy as described previously (27). Insulin induced membrane ruffling which was visible as an irregular rim along a part or around all of the margin of the cells (Fig. 1A). The insulin-induced membrane ruffling was detectable within 2 min, reached maximum at 5 min, and decreased within 30 min after the addition of insulin (Fig. 1A). These results are consistent with earlier observations (20, 27, 34). HGF also induced membrane ruffling, but its morphology was different from that of the insulin-induced kind (Fig. 1B). The HGF-induced membrane ruffling was visible as curtain-like folds or irregular spikes dispersed around the cell surface and was detectable within 2 min, reached maximum at 10 min, and decreased but continued at least for 1 h after the addition of HGF (Fig. 1B). Both growth factor-induced membrane rufflings were morphologically different from each other until they disappeared (Fig. 1). In this series of experiments, 1×10^{-6} M insulin and 5×10^{-11} M HGF were used. When higher levels of insulin ($5 \times$

10^{-6} M) and HGF (2×10^{-10} M) were used, results the same as those shown in Fig. 1 were obtained (data not shown).

Effect of *rho* GDI and C3 on the insulin- and HGF-induced membrane rufflings. Insulin and HGF induced maximal membrane rufflings at 5 and 10 min, respectively, after the addition of each growth factor as described above (Fig. 2, panels a), and both of these rufflings were inhibited by microinjection of *rho* GDI into the cells (Fig. 2, panels b). Moreover, the HGF-induced membrane ruffling was also inhibited by microinjection with C3 into the cells (Fig. 2Bc). However, the insulin-induced membrane ruffling was not inhibited by microinjection with C3 (Fig. 2Ac). The inhibitory action of C3 on the HGF-induced membrane ruffling was prevented by comicroinjection with GTPγS-bound *rho*A p21 mutant (*rho*A^{Ile-41} p21) (Fig. 2Bd) but not with GTPγS-bound normal *rho*A p21 (data not shown). *rho*A^{Ile-41} p21 is not ADP-ribosylated by C3 because of the substitution of Ile-41 for Asn at the ADP-ribosylation site. The inability of normal *rho*A p21 to prevent the C3 action might be due to the ADP-ribosylation by C3 of the microinjected as well as endogenous *rho* p21s.

We have previously shown that *rho* GDI is active on *rho*A p21 and *rac*1 p21 and interacts with the GDP-bound form of each small G protein much more preferentially than with the GTP-bound form (48, 56). The inhibitory action of *rho* GDI in insulin-induced membrane ruffling was prevented by comicroinjection with GTPγS-bound *rac*1 p21, and membrane ruffling morphologically similar to the insulin-induced kind was observed (Fig. 3Ac). Membrane ruffling was also visible by comicroinjection of *rho* GDI with GTPγS-bound *rho*A p21, but its morphology was apparently different from that of the insulin-induced kind (Fig. 3Ab). The inhibitory action of *rho* GDI in HGF-induced membrane ruffling was prevented by comicroinjection with GTPγS-bound *rho*A p21, and membrane ruffling morphologically similar to the HGF-induced kind was observed (Fig. 3Bb). The membrane ruffling was also visible by comicroinjection of *rho* GDI with GTPγS-bound *rac*1 p21, but its morphology was apparently different from that of the HGF-induced kind and was similar to the insulin-induced kind (Fig. 3Bc).

***rac*1 p21- and *rho*A p21-induced membrane rufflings.** Microinjection of either GTPγS-bound *rac*1 p21 or *rho*A p21 alone induced membrane ruffling (Fig. 4B and C). The morphology of the *rac*1 p21-induced membrane ruffling was similar to that of the insulin-induced kind, but its intensity was slightly weaker than that of the insulin-induced kind (Fig. 1A and 4C). This membrane ruffling was detectable within 10 min and decreased within 30 min after the microinjection. The intensity of the membrane ruffling was not very changeable until it disappeared. The morphology of the *rho*A p21-induced membrane ruffling was apparently different from those of the both insulin- and HGF-induced kinds and was visible as weak flat folds along all of the margin of the cells (Fig. 1 and 4B). The time course of the *rho*A p21-induced membrane ruffling was similar to that of the *rac*1 p21-induced kind. The intensity of the membrane ruffling was also not very changeable until it disappeared. In this series of experiments, 1 mg of *rho*A p21 per ml and 1 mg of *rac*1 p21 per ml were microinjected. When higher levels of *rho*A p21 and *rac*1 p21 (3 mg/ml) were used, results the same as those shown in Fig. 4B and C were obtained (data not shown).

Inability of *ras* p21 to induce membrane ruffling. It has been reported that microinjection of a dominant active Ha-*ras* p21 (Ha-*ras*$^{Val-12}$ p21) alone induces membrane ruffling of the rat embryo fibroblast (8). Moreover, insulin and HGF have been shown to activate *ras* p21 in several types of cells, such as NIH 3T3 cells and A549 cells (11, 22). However, microinjection of Ki-*ras*$^{Val-12}$ p21 alone into KB cells did not induce membrane ruffling (Fig. 4D). This dominant active mutant of Ki-*ras* p21 induced DNA synthesis in Swiss 3T3 cells as described previously (58). Moreover, microinjection of a dominant negative Ki-*ras* p21 mutant (Ki-*ras*$^{Asn-17}$ p21) into KB cells did not inhibit insulin- or HGF-induced membrane ruffling (Fig. 5B).

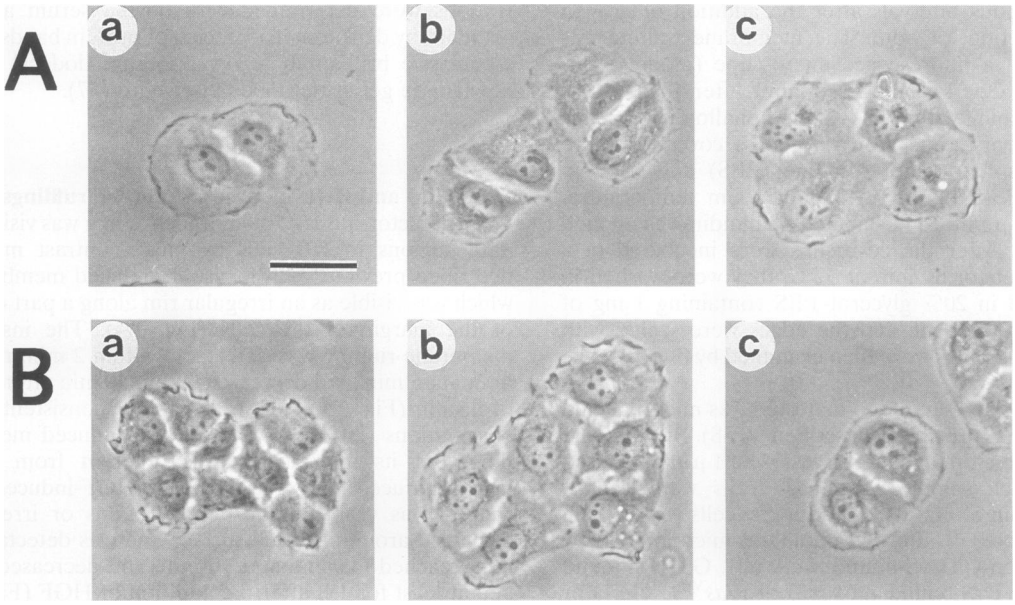

FIG. 3. Prevention of *rho* GDI action by *rho*A p21 or *rac*1 p21. KB cells were microinjected with buffer A (a), *rho* GDI plus GTPγS-bound *rho*A p21 (b), or *rho* GDI plus GTPγS-bound *rac*1 p21 (c). At 30 min after microinjection, KB cells were stimulated with 1×10^{-6} M insulin (A) or 5×10^{-11} M HGF (B). Photographs were taken 5 min after stimulation with insulin and 10 min after stimulation with HGF. The results shown are representative of three independent experiments. Bar, 20 μm. All photographs were taken with the same magnification.

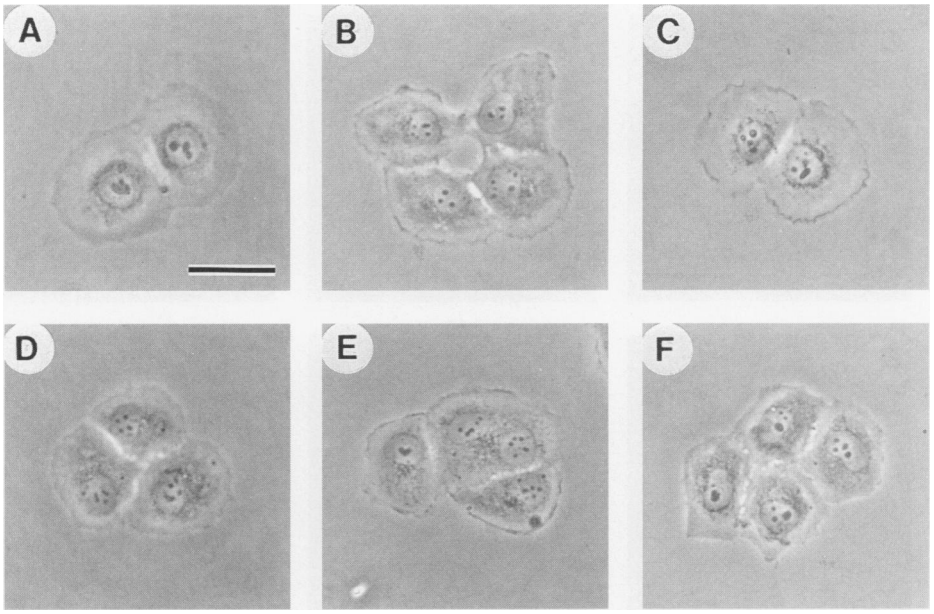

FIG. 4. *rho*A p21- and *rac*1 p21-induced membrane rufflings. KB cells were microinjected with buffer A (A), GTPγS-bound *rho*A p21 (B), GTPγS-bound *rac*1 p21 (C), or Ki-*ras*$^{Val-12}$ p21 (D) or were stimulated with 1×10^{-7} M TPA (E) or 5×10^{-8} M ionomycin (F). Photographs were taken 20 min after microinjection or stimulation. The results shown are representative of three independent experiments. Bar, 20 μm. All photographs were taken with the same magnification.

TPA-induced membrane ruffling and effect of *rho* GDI and C3 on it. HGF has been reported to stimulate phospholipase C-γ activation, leading to formation of two second messengers, diacylglycerol, which activates PKC, and inositol triphosphate, which mobilizes intracellular Ca^{2+} (40). Therefore, we next investigated the effect of TPA, a PKC-activating phorbol ester, and a Ca^{2+} ionophore, ionomycin, on membrane ruffling of KB cells. TPA induced membrane ruffling, but ionomycin did not (Fig. 4E and F). TPA-induced membrane ruffling was also inhibited by microinjection of *rho* GDI or C3 (Fig. 6B and C). The inhibitory action of *rho* GDI in TPA-induced membrane ruffling was prevented by comicroinjection with GTPγS-bound *rho*A p21 (Fig. 6D) but not with GTPγS-bound *rac*1 p21 (data not shown). Moreover, the inhibitory action of C3 on TPA-induced membrane ruffling was prevented by comicroinjection with GTPγS-bound *rho*A p21 mutant (*rho*A^{Ile-41} p21) (Fig. 6E).

Different organization of actin in various membrane rufflings. To investigate the organization of actin in various types of membrane rufflings, KB cells were stained with FITC-labeled phalloidin, which binds specifically to F-actin (Fig. 7). Insulin-induced membrane ruffling, which was visible as an irregular rim along a part or around all of the margin of the cells by phase-contrast microscopy (Fig. 7Ab), and the HGF-induced kind, which was visible as curtain-like folds or irregular spikes dispersed around the cell surface by phase-contrast microscopy (Fig. 7Ac), were confirmed by phalloidin staining (Fig. 7Bb and c). Phalloidin staining of HGF-induced membrane ruffling was different from that of the insulin-induced kind (Fig. 7Bb and c). TPA-induced membrane ruffling, which was visible as flat and smooth folds around all of the margin of the cells by phase-contrast microscopy (Fig. 7Ad), was also confirmed by phalloidin staining (Fig. 7, Bd). Phalloidin staining of TPA-induced membrane ruffling was apparently different from that of the insulin- and HGF-induced kinds, although the morphology of the TPA-induced membrane ruffling was not clearly distinguishable from that of the insulin-induced kind by phase-contrast microscopy (Fig. 7, panels b and d). *rho*A p21-induced membrane ruffling, which was visible as weak flat folds by phase-contrast microscopy (Fig. 7Ae), was similarly observed by phalloidin staining (Fig. 7Be). Phalloidin staining of the *rho*A p21-induced membrane ruffling was apparently different from that of the insulin- and HGF-induced kinds but similar to the TPA-induced kind (Fig. 7Bd and e). However, its intensity was slightly weaker than that of TPA-induced ruffling. *rac*1 p21-induced membrane ruffling, which was similar to the insulin-induced kind by phase-contrast microscopy (Fig. 7Ab and f), was also similarly observed by phalloidin staining (Fig. 7Bb and f). However, its intensity was slightly weaker than that of the insulin-induced kind. In this series of experiments, cells were fixed and stained with FITC-phalloidin at various intervals after the addition of growth factors or microinjection, but until each membrane ruffling disappeared, their phalloidin stainings were characteristic of each growth factor- and each small G protein-induced membrane ruffling (data not shown).

DISCUSSION

KB cells have been reported to form striking membrane rufflings in response to insulin, insulin-like growth factor I, and EGF (20, 26, 27, 34). Insulin- and insulin-like growth factor I-induced membrane rufflings are morphologically same, but insulin- and EGF-induced membrane rufflings are apparently different (34). We have first shown here that HGF also induces membrane ruffling in KB cells. The morphology of HGF-induced membrane ruffling is different from that of the insulin-induced kind. This difference is confirmed by F-actin staining with FITC-phalloidin. These results suggest that each growth factor triggers a different signal cascade, which is related to morphologically different membrane ruffling. EGF-induced membrane ruffling was morphologically similar to the HGF-

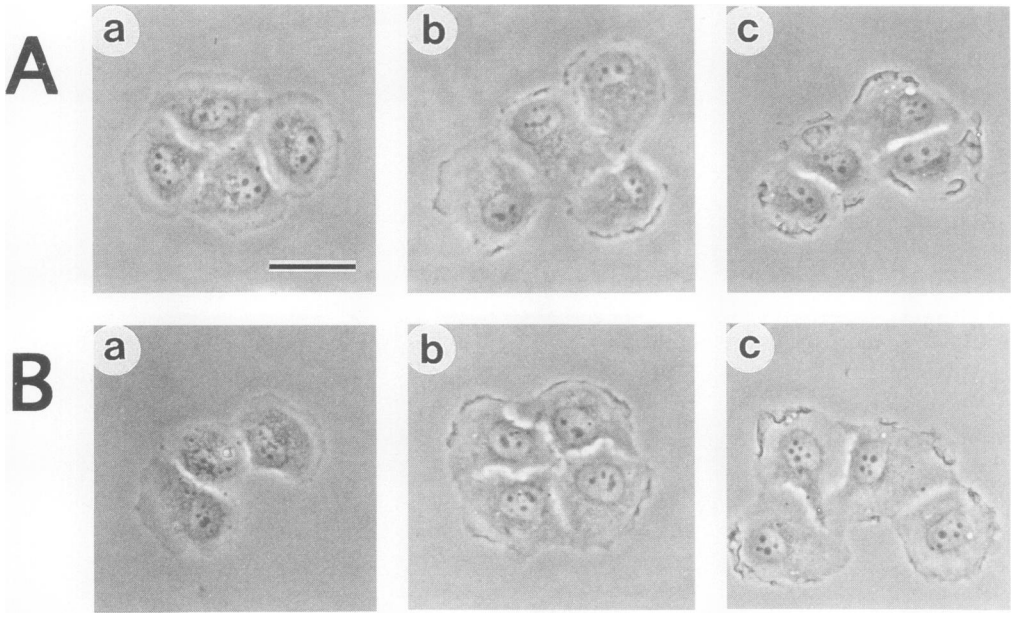

FIG. 5. Effect of Ki-*ras*$^{Asn-17}$ p21 on insulin- and HGF-induced membrane rufflings. KB cells were microinjected with buffer A (A) or Ki-*ras*$^{Asn-17}$ p21 (B). At 30 min after microinjection, KB cells were stimulated with nothing (a), 1×10^{-6} M insulin (b), or 5×10^{-11} M HGF (c). Photographs were taken 5 min after stimulation with insulin and 10 min after stimulation with HGF. The results shown are representative of three independent experiments. Bar, 20 μm. All photographs were taken with the same magnification.

induced kind, but we have not shown here the result of this membrane ruffling, because we could not always obtain consistent results in EGF-induced membrane ruffling.

We have then shown here that insulin-induced membrane ruffling is inhibited by microinjection of *rho* GDI but not by microinjection of C3. The *rho* GDI action is prevented by comicroinjection with GTPγS-bound *rac*1 p21, and membrane ruffling morphologically similar to the insulin-induced kind is observed. Membrane ruffling is also visible by comicroinjection of *rho* GDI with GTPγS-bound *rho*A p21, but its morphology is apparently different from that of the insulin-induced kind and similar to that induced by microinjection of GTPγS-bound *rho*A p21 alone or by TPA (see below). These results indicate that *rac*1 p21, but not *rho*A p21, is involved in insulin-induced

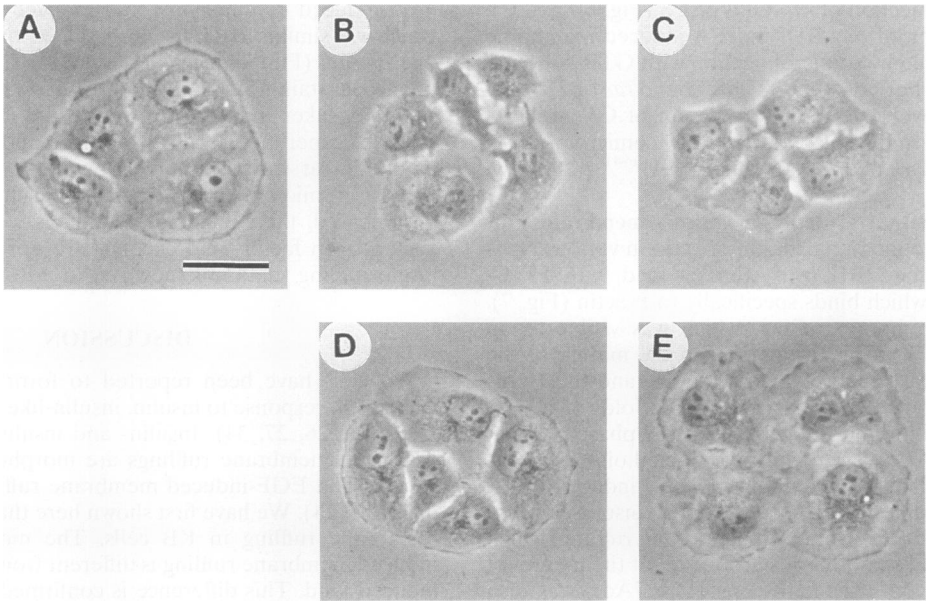

FIG. 6. Inhibition of TPA-induced membrane ruffling by microinjection of *rho* GDI or C3 into KB cells. KB cells were microinjected with buffer A (A), *rho* GDI (B), C3 (C), *rho* GDI plus GTPγS-bound *rho*A p21 (D), or C3 plus GTPγS-bound *rho*A^{Ile-41} p21 (E). At 30 min after microinjection, KB cells were stimulated with 10^{-7} M TPA. Photographs were taken 20 min after stimulation with TPA. The results shown are representative of three independent experiments. Bar, 20 μm. All photographs were taken with the same magnification.

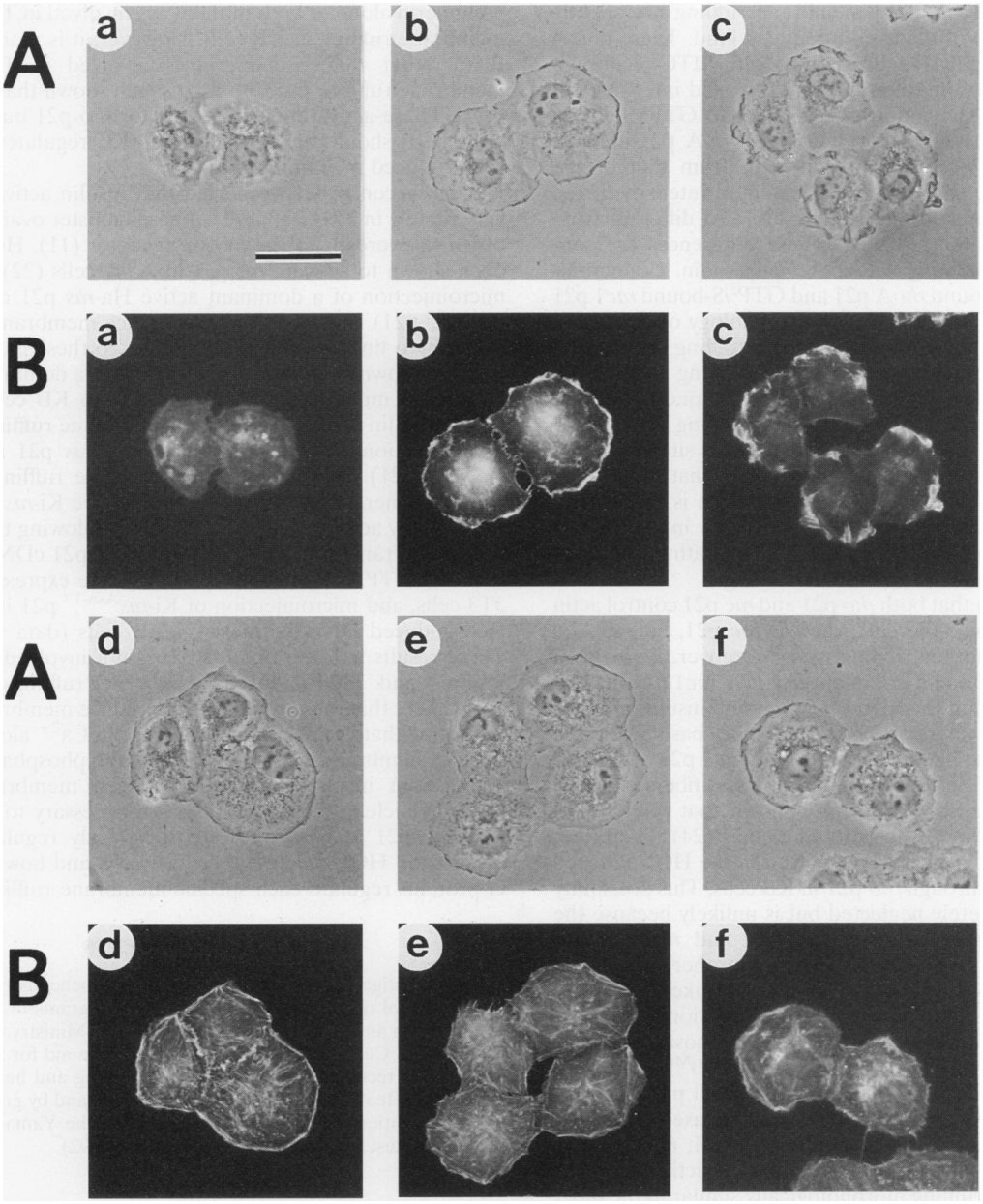

FIG. 7. Different organization of actin in various membrane rufflings. KB cells were stimulated with nothing (a), 1×10^{-6} M insulin (b), 5×10^{-11} M HGF (c), or 1×10^{-7} M TPA (d) or microinjected with GTPγS-bound *rho*A p21 (e) or GTPγS-bound *rac*1 p21 (f). Photographs were taken 5 min after stimulation with insulin, 10 min after stimulation with HGF, 20 min after stimulation with TPA, or 20 min after microinjection. After the cells were analyzed by phase-contrast microscopy (A), they were fixed, stained with FITC-labeled phalloidin, and analyzed by fluorescence microscopy (B). The results shown are representative of three independent experiments. Bar, 20 μm. All photographs were taken with the same magnification.

membrane ruffling and are consistent with the earlier observations that *rac*1 p21, but not *rho*A p21, is involved in insulin-induced membrane ruffling in Swiss 3T3 cells (43). In contrast, HGF-induced membrane ruffling is inhibited by microinjection of *rho* GDI and C3. The *rho* GDI action is prevented by comicroinjection with GTPγS-bound *rho*A p21, and membrane ruffling morphologically similar to the HGF-induced kind is observed. Membrane ruffling is also visible by comicroinjection of *rho* GDI with GTPγS-bound *rac*1 p21, but its morphology is apparently different from that of the HGF-induced kind and similar to that of the insulin-induced kind. Moreover, C3 action is prevented by comicroinjection with GTPγS-bound *rho*A$^{Ile\text{-}41}$ p21, which is resistant to the C3 action. These results indicate that *rho*A p21, but not *rac*1 p21, is involved in HGF-induced membrane ruffling and are consistent with our earlier observations that *rho*A p21, but not *rac*1 p21, is involved in HGF-induced cell motility in mouse keratinocytes (54).

We have moreover shown here that microinjection of either GTPγS-bound *rac*1 p21 or *rho*A p21 alone induces membrane ruffling. *rac*1 p21-induced membrane ruffling is morphologically similar to the insulin-induced kind and apparently different from the HGF-induced kind, although the time course and

intensity of *rac*1 p21-induced membrane ruffling are slightly different from those of the insulin-induced kind. These differences are confirmed by F-actin staining with FITC-phalloidin and might be due to the different durations and intensities of the insulin-induced activation of *rac* p21 and GTPγS-bound *rac*1 p21. In contrast, the morphology of *rho*A p21-induced membrane ruffling is apparently different from that of the HGF-induced kind, and the time course and intensity of the *rho*A p21-induced membrane ruffling are also different from those of the HGF-induced kind. These differences are confirmed by F-actin staining with FITC-phalloidin. Comicroinjection of GTPγS-bound *rho*A p21 and GTPγS-bound *rac*1 p21 induced membrane ruffling, but the morphology of this membrane ruffling was not similar to that of ruffling induced by HGF and was rather similar to that of ruffling induced by microinjection of GTPγS-bound *rac*1 p21 alone (data not shown). The reason why the membrane ruffling induced by comicroinjection of *rho*A p21 and *rac*1 p21 was similar to that induced by *rac*1 p21 alone and not similar to that induced by *rho*A p21 alone or different from both of them is not known, but these results indicate that another pathway in addition to the *rho* p21 pathway, which is not the *rac* p21 pathway, may be involved in HGF-induced membrane ruffling.

It has been shown that both *rho* p21 and *rac* p21 control actin stress fibers in Swiss 3T3 cells, whereas *rac* p21, but not *rho* p21, regulates membrane ruffling (43). Moreover, it has been shown that both C3 and a dominant negative *rac*1 p21 mutant (*rac*1^{Asn-17} p21) inhibit the PDGF-, EGF-, and insulin-induced increase in stress fibers (42, 43). On the basis of these observations, it has been proposed that *rac* p21 is placed upstream of *rho* p21 in the regulation of stress fibers (43). On the other hand, we have previously shown that *rho* GDI is active not only on *rho* p21 but also on *rac* p21 (24). Therefore, it is possible that *rac* p21 is also involved in the HGF-induced membrane ruffling through *rho* p21 in KB cells. This possibility could not be completely neglected but is unlikely because the membrane rufflings induced by *rho* p21 and *rac* p21 are morphologically slightly different from each other.

The insulin receptor has been shown to be linked to at least two signal pathways in a tyrosine phosphorylation-dependent manner: a *ras* p21 pathway and a phosphatidylinositol 3-kinase pathway (11, 18, 46). The HGF receptor, p190^{Met}, has been shown to be linked not only to these two signal pathways but also to an additional pathway of phospholipase C-γ which leads to PKC activation and Ca^{2+} mobilization (21, 22, 40). Consistently, we have shown here that PKC-activating TPA induces membrane ruffling morphologically similar to the *rho*A p21-induced kind. This similarity is confirmed by F-actin staining with FITC-phalloidin. Moreover, we have shown here that the TPA-induced membrane ruffling is inhibited by microinjection of *rho* GDI or C3, indicating that *rho* p21 and *rho* GDI are also involved in TPA-induced membrane ruffling. These results are consistent with the recent observations that thrombin- and TPA-induced aggregation of platelets and TPA-induced, lymphocyte function-associated antigen 1-dependent aggregation of lymphocytes are inhibited by pretreatment with C3 (36, 55) and also with our recent observation that the TPA-induced cell motility of mouse keratinocytes is inhibited by microinjection of *rho* GDI or C3 (54).

TPA is well known to be a direct activator of PKC (13). TPA binds to the C1 domain of PKC. However, recent studies have clarified that several proteins other than PKC, such as *n*-chimerin, Bcr, Raf, diacylglycerol kinase, and Vav, have homologous regions of the C1 domain (3–5, 9, 16, 28, 49). Actually, *n*-chimerin has been reported to be one of the target molecules for TPA. Therefore, it is possible that PKC or *n*-chimerin alone or both of them are involved in TPA-induced membrane ruffling in KB cells. However, it is more likely that PKC rather than *n*-chimerin is involved in TPA-induced membrane ruffling, because it has been shown that *n*-chimerin is a GTPase-activating protein not for *rho* p21 but mainly for *rac* p21. It should be clarified how PKC regulates *rho* p21 in TPA-induced membrane ruffling.

It has recently been reported that insulin activates *ras* p21 very rapidly in NIH 3T3 and Chinese hamster ovary cells, both of which overexpress the insulin receptor (11). HGF has also been shown to activate *ras* p21 in A549 cells (22). Moreover, microinjection of a dominant active Ha-*ras* p21 mutant (Ha-*ras*$^{Val-12}$ p21) has been shown to induce membrane ruffling of rat embryo fibroblasts (8). In contrast to these earlier results, we have shown here that microinjection of a dominant negative Ki-*ras* p21 mutant (Ki-*ras*$^{Asn-17}$ p21) into KB cells does not inhibit insulin- and HGF-induced membrane rufflings and that microinjection of a dominant active Ki-*ras* p21 mutant (Ki-*ras*$^{Val-12}$ p21) does not induce membrane ruffling. We have confirmed here that this dominant negative Ki-*ras*$^{Asn-17}$ p21 is functionally active in intact cells by the following two different methods. Transfection of the Ki-*ras*$^{Asn-17}$ p21 cDNA inhibited PDGF- or TPA-stimulated c-*fos*-luciferase expression in NIH 3T3 cells, and microinjection of Ki-*ras*$^{Asn-17}$ p21 inhibited the EGF-induced DNA synthesis in KB cells (data not shown). These results indicate that *ras* p21 is not involved in both the insulin- and HGF-induced membrane rufflings. We have shown here that ionomycin does not induce membrane ruffling, indicating that the continuous increase in Ca^{2+} alone does not induce membrane ruffling. The role of phosphatidylinositol 3-kinase in insulin- and HGF-induced membrane ruffling remains unclear. Further studies are necessary to understand how *rac* p21 and *rho* p21 are specifically regulated by the insulin and HGF receptors, respectively, and how these small G proteins regulate each specific membrane ruffling.

ACKNOWLEDGMENTS

This investigation at the Department of Biochemistry, Kobe University School of Medicine, was supported by grants-in-aid for scientific research and for cancer research from the Ministry of Education, Science, and Culture, Japan (1992); by grants-in-aid for abnormalities in hormone receptor mechanisms and for aging and health from the Ministry of Health and Welfare, Japan (1992); and by grants from the Human Frontier Science Program (1992) and the Yamanouchi Foundation for Research on Metabolic Disease (1992).

REFERENCES

1. **Abercrombie, M., J. E. M. Heaysman, and S. M. Pegrum.** 1970. The locomotion of fibroblasts in culture. II. "Ruffling." Exp. Cell Res. **60:**437–444.
2. **Abo, A., E. Pick, A. Hall, N. Totty, C. G. Teahan, and A. W. Segal.** 1991. Activation of the NADPH oxidase involves the small GTP-binding protein p21^{rac1}. Nature (London) **353:**668–670.
3. **Ahmed, S., R. Kozma, J. Lee, C. Monfries, N. Harden, and L. Lim.** 1991. The cysteine-rich domain of human proteins, neuronal chimaerin, protein kinase C and diacylglycerol kinase binds zinc: evidence for the involvement of a zinc-dependent structure in phorbol ester binding. Biochem. J. **280:**233–241.
4. **Ahmed, S., R. Kozma, C. Monfries, C. Hall, H. H. Lim, P. Smith, and L. Lim.** 1990. Human brain *n*-chimaerin cDNA encodes a novel phorbol ester receptor. Biochem. J. **272:**767–773.
5. **Ahmed, S., J. Lee, R. Kozma, A. Best, C. Monfries, and L. Lim.** 1993. A novel functional target for tumor-promoting phorbol esters and lysophosphatidic acid: the p21*rac*-GTPase activating protein *n*-chimaerin. J. Biol. Chem. **268:**10709–10712.
6. **Aktories, K., S. Rösener, U. Blaschke, and G. Chhatwal.** 1988. Botulinum ADP-ribosyltransferase C3: purification of the enzyme and characterization of the ADP-ribosylation reaction in platelet

membranes. Eur. J. Biochem. **172:**445–450.

7. **Ando, S., K. Kaibuchi, T. Sasaki, K. Hiraoka, T. Nishiyama, T. Mizuno, M. Asada, H. Nunoi, I. Matsuda, Y. Matsuura, P. Polakis, F. McCormick, and Y. Takai.** 1992. Post-translational processing of *rac* p21s is important both for their interaction with the GDP/GTP exchange proteins and for their activation of NADPH oxidase. J. Biol. Chem. **267:**25709–25713.
8. **Bar-Sagi, D., and J. R. Feramisco.** 1986. Induction of membrane ruffling and fluid-phase pinocytosis in quiescent fibroblasts by *ras* proteins. Science **233:**1061–1068.
9. **Beck, T. W., M. Huleihel, M. Gunnel, T. I. Bonner, and U. R. Rapp.** 1987. The complete coding sequence of the human A-*raf*-1 oncogene and transforming activity of a human A-*raf* carrying retrovirus. Nucleic Acids Res. **15:**595–609.
10. **Braun, U., B. Habermann, I. Just, K. Aktories, and J. Vandekerckhove.** 1989. Purification of the 22 kDa protein substrate of botulinum ADP-ribosyltransferase C3 from porcine brain cytosol and its characterization as a GTP-binding protein highly homologous to the *rho* gene product. FEBS Lett. **243:**70–76.
11. **Burgering, B. M. T., R. H. Medema, J. A. Maassen, M. L. Van de Wetering, and A. J. Van der Eb.** 1991. Insulin stimulation of gene expression mediated by p21*ras* activation. EMBO J. **10:**1103–1109.
12. **Cantley, L. C., K. R. Auger, C. Carpenter, B. Duckworth, A. Graziani, R. Kapeller, and S. Soltoff.** 1991. Oncogenes and signal transduction. Cell **64:**281–302.
13. **Castagna, M., Y. Takai, K. Kaibuchi, K. Sano, U. Kikkawa, and Y. Nishizuka.** 1982. Direct activation of calcium-activated, phospholipid-dependent protein kinase by tumor-promoting phorbol esters. J. Biol. Chem. **257:**7847–7851.
14. **Chardin, P., P. Boquet, P. Madaule, M. R. Popoff, E. J. Rubin, and D. M. Gill.** 1989. The mammalian G protein *rho*C is ADP-ribosylated by *Clostridium botulinum* exoenzyme C3 and affects actin microfilaments in Vero cells. EMBO J. **8:**1087–1092.
15. **Didsbury, J., R. F. Weber, G. M. Bokoch, T. Evans, and R. Snyderman.** 1989. *rac*, a novel *ras*-related family of proteins that are botulinum toxin substrates. J. Biol. Chem. **264:**16378–16382.
16. **Diekmann, D., S. Brill, M. D. Garrett, N. Totty, J. Hsuan, C. Monfries, C. Hall, L. Lim, and A. Hall.** 1991. *Bcr* encodes a GTPase-activating protein for p21^{rac}. Nature (London) **351:**400–402.
17. **Dipasquale, A.** 1975. Locomotory activity of epithelial cells in culture. Exp. Cell Res. **94:**191–215.
18. **Endemann, G., K. Yonezawa, and R. A. Roth.** 1990. Phosphatidylinositol kinase or an associated protein is a substrate for the insulin receptor tyrosine kinase. J. Biol. Chem. **265:**396–400.
19. **Fukumoto, Y., K. Kaibuchi, Y. Hori, H. Fujioka, S. Araki, T. Ueda, A. Kikuchi, and Y. Takai.** 1990. Molecular cloning and characterization of a novel type of regulatory protein (GDI) for the *rho* proteins, *ras* p21-like small GTP-binding proteins. Oncogene **5:**1321–1328.
20. **Goshima, K., A. Masuda, and K. Owaribe.** 1984. Insulin-induced formation of ruffling membranes of KB cells and its correlation with enhancement of amino acid transport. J. Cell Biol. **98:**801–809.
21. **Graziani, A., D. Gramaglia, L. C. Cantley, and P. M. Comoglio.** 1991. The tyrosine-phosphorylated hepatocyte growth factor/scatter factor receptor associates with phosphatidylinositol 3-kinase. J. Biol. Chem. **266:**22087–22090.
22. **Graziani, A., D. Gramaglia, P. D. Zonca, and P. M. Comoglio.** 1993. Hepatocyte growth factor/scatter factor stimulates the ras-guanine nucleotide exchanger. J. Biol. Chem. **268:**9165–9168.
23. **Hall, A.** 1990. The cellular functions of small GTP-binding proteins. Science **249:**635–640.
24. **Hiraoka, K., K. Kaibuchi, S. Ando, T. Musha, K. Takaishi, T. Mizuno, M. Asada, L. Ménard, E. Tomhave, J. Didsbury, R. Snyderman, and Y. Takai.** 1992. Both stimulatory and inhibitory GDP/GTP exchange proteins, *smg* GDS and *rho* GDI, are active on multiple small GTP-binding proteins. Biochem. Biophys. Res. Commun. **182:**921–930.
25. **Hirata, K., A. Kikuchi, T. Sasaki, S. Kuroda, K. Kaibuchi, Y. Matsuura, H. Seki, K. Saida, and Y. Takai.** 1992. Involvement of *rho* p21 in the GTP-enhanced calcium ion sensitivity of smooth muscle contraction. J. Biol. Chem. **267:**8719–8722.
26. **Izumi, T., Y. Saeki, Y. Akanuma, F. Takaku, and M. Kasuga.** 1988. Requirement for receptor-intrinsic tyrosine kinase activities during ligand-induced membrane ruffling of KB cells: essential sites of src-related growth factor receptor kinases. J. Biol. Chem. **263:**10386–10393.
27. **Kadowaki, T., S. Koyasu, E. Nishida, H. Sakai, F. Takaku, I. Yahara, and M. Kasuga.** 1986. Insulin-like growth factors, insulin, and epidermal growth factor cause rapid cytoskeletal reorganization in KB cells: clarification of the roles of type I insulin-like growth factor receptors and insulin receptors. J. Biol. Chem. **261:**16141–16147.
28. **Katzav, S., D. Martin-Zanca, and M. Barbacid.** 1989. *vav*, a novel human oncogene derived from a locus ubiquitously expressed in hematopoietic cells. EMBO J. **8:**2283–2290.
29. **Kikuchi, A., K. Yamamoto, T. Fujita, and Y. Takai.** 1988. ADP-ribosylation of the bovine brain *rho* protein by botulinum toxin type C1. J. Biol. Chem. **263:**16303–16308.
30. **Kishi, K., T. Sasaki, S. Kuroda, T. Itoh, and Y. Takai.** 1993. Regulation of cytoplasmic division of *Xenopus* embryo by *rho* p21 and its inhibitory GDP/GTP exchange protein (*rho* GDI). J. Cell Biol. **120:**1187–1195.
31. **Knaus, U. G., P. G. Heyworth, T. Evans, J. T. Curnutte, and G. M. Bokoch.** 1991. Regulation of phagocyte oxygen radical production by the GTP-binding protein rac2. Science **254:**1512–1515.
32. **Mellström, K., C.-H. Heldin, and B. Westermark.** 1988. Induction of circular membrane ruffling on human fibroblasts by platelet-derived growth factor. Exp. Cell Res. **177:**347–359.
33. **Miura, Y., A. Kikuchi, T. Musha, S. Kuroda, H. Yaku, T. Sasaki, and Y. Takai.** 1993. Regulation of morphology by *rho* p21 and its inhibitory GDP/GTP exchange protein (*rho* GDI) in Swiss 3T3 cells. J. Biol. Chem. **268:**510–515.
34. **Miyata, Y., E. Nishida, and H. Sakai.** 1988. Growth factor- and phorbol ester-induced changes in cell morphology analyzed by digital image processing. Exp. Cell Res. **175:**286–297.
35. **Mizuno, T., K. Kaibuchi, S. Ando, T. Musha, K. Hiraoka, K. Takaishi, M. Asada, H. Nunoi, I. Matsuda, and Y. Takai.** 1992. Regulation of the superoxide-generating NADPH oxidase by small GTP-binding protein and its stimulatory and inhibitory GDP/GTP exchange proteins. J. Biol. Chem. **267:**10215–10218.
36. **Morii, N., T. Teru-uchi, T. Tominaga, N. Kumagai, S. Kozaki, F. Ushikubi, and S. Narumiya.** 1992. A *rho* gene product in human blood platelets. II. Effects of the ADP-ribosylation by botulinum C3 ADP-ribosyltransferase on platelet aggregation. J. Biol. Chem. **267:**20921–20926.
37. **Nakamura, T., T. Nishizawa, M. Hagiya, T. Seki, M. Shimonishi, A. Sugimura, K. Tashiro, and S. Shimizu.** 1989. Molecular cloning and expression of human hepatocyte growth factor. Nature (London) **342:**440–443.
38. **Narumiya, S., A. Sekine, and M. Fujiwara.** 1988. Substrate for botulinum ADP-ribosyltransferase, Gb, has an amino acid sequence homologous to a putative *rho* gene product. J. Biol. Chem. **263:**17255–17257.
39. **Nemoto, Y., T. Namba, S. Kozaki, and S. Narumiya.** 1991. *Clostridium botulinum* C3 ADP-ribosyltransferase gene: cloning, sequencing, and expression of a functional protein in *Escherichia coli*. J. Biol. Chem. **266:**19312–19319.
40. **Okano, Y., K. Mizuno, S. Osada, T. Nakamura, and Y. Nozawa.** 1993. Tyrosine phosphorylation of phospholipase Cγ in c-*met*/HGF receptor-stimulated hepatocytes: comparison with HepG2 hepatocarcinoma cells. Biochem. Biophys. Res. Commun. **190:**842–848.
41. **Paterson, H. F., A. J. Self, M. D. Garrett, I. Just, K. Aktories, and A. Hall.** 1990. Microinjection of recombinant p21^{rho} induces rapid changes in cell morphology. J. Cell Biol. **111:**1001–1007.
42. **Ridley, A. J., and A. Hall.** 1992. The small GTP-binding protein rho regulates the assembly of focal adhesions and actin stress fibers in response to growth factors. Cell **70:**389–399.
43. **Ridley, A. J., H. F. Paterson, C. L. Johnston, D. Diekmann, and A. Hall.** 1992. The small GTP-binding protein rac regulates growth factor-induced membrane ruffling. Cell **70:**401–410.
44. **Rotrosen, D., C. L. Yeung, T. L. Leto, H. L. Malech, and C. H. Kwong.** 1992. Cytochrome b_{558}: the flavin-binding component of the phagocyte NADPH oxidase. Science **256:**1459–1462.

45. **Rubin, E. J., D. M. Gill, P. Boquet, and M. R. Popoff.** 1988. Functional modification of a 21-kilodalton G protein when ADP-ribosylated by exoenzyme C3 of *Clostridium botulinum*. Mol. Cell. Biol. **8:**418–426.
46. **Ruderman, N. B., R. Kapeller, M. F. White, and L. C. Cantley.** 1990. Activation of phosphatidylinositol 3-kinase by insulin. Proc. Natl. Acad. Sci. USA **87:**1411–1415.
47. **Sambrook, J., E. F. Fritsch, and T. Maniatis.** 1989. Molecular cloning: a laboratory manual, 2nd ed. Cold Spring Harbor Laboratory Press, Cold Spring Harbor, N.Y.
48. **Sasaki, T., M. Kato, and Y. Takai.** 1993. Consequences of weak interaction of *rho* GDI with the GTP-bound forms of *rho* p21 and *rac* p21. J. Biol. Chem. **268:**23959–23963.
49. **Schaap, D., J. de Widt, J. van der Wal, J. Vandekerckhove, J. van Damme, D. Gussow, H. L. Ploegh, W. J. van Blitterswijk, and R. L. van der Bend.** 1990. Purification, cDNA-cloning and expression of human diacylglycerol kinase. FEBS Lett. **275:**151–158.
50. **Sekine, A., M. Fujiwara, and S. Narumiya.** 1989. Asparagine residue in the *rho* gene product is the modification site for botulinum ADP-ribosyltransferase. J. Biol. Chem. **264:**8602–8605.
51. **Smith, D. B., and K. S. Johnson.** 1988. Single-step purification of polypeptides expressed in *Escherichia coli* as fusions with glutathione S-transferase. Gene **67:**31–40.
52. **Takai, Y., K. Kaibuchi, A. Kikuchi, and M. Kawata.** 1992. Small GTP-binding proteins. Int. Rev. Cytol. **133:**187–230.
53. **Takaishi, K., A. Kikuchi, S. Kuroda, K. Kotani, T. Sasaki, and Y. Takai.** 1993. Involvement of *rho* p21 and its inhibitory GDP/GTP exchange protein (*rho* GDI) in cell motility. Mol. Cell. Biol. **13:**72–79.
54. **Takaishi, K., T. Sasaki, M. Kato, W. Yamochi, S. Kuroda, T. Nakamura, M. Takeichi, and Y. Takai.** 1994. Involvement of *Rho* p21 small GTP-binding protein and its regulator in the HGF-induced cell motility. Oncogene **9:**273–279.
55. **Tominaga, T., K. Sugie, M. Hirata, N. Morii, J. Fukata, A. Uchida, H. Imura, and S. Narumiya.** 1993. Inhibition of PMA-induced, LFA-1-dependent lymphocyte aggregation by ADP ribosylation of the small molecular weight GTP binding protein, *rho*. J. Cell Biol. **120:**1529–1537.
56. **Ueda, T., A. Kikuchi, N. Ohga, J. Yamamoto, and Y. Takai.** 1990. Purification and characterization from bovine brain cytosol of a novel regulatory protein inhibiting the dissociation of GDP from and the subsequent binding of GTP to *rho*B p20, a *ras* p21-like GTP-binding protein. J. Biol. Chem. **265:**9373–9380.
57. **Weber, K., J. R. Pringle, and M. Osborn.** 1972. Measurement of molecular weights by electrophoresis on SDS-acrylamide gel. Methods Enzymol. **26:**3–27.
58. **Yoshida, Y., M. Kawata, Y. Miura, T. Musha, T. Sasaki, A. Kikuchi, and Y. Takai.** 1992. Microinjection of *smg/rap*1/K*rev*-1 p21 into Swiss 3T3 cells induces DNA synthesis and morphological changes. Mol. Cell. Biol. **12:**3407–3414.